A Chemical Ionization Mass Spectrometer for Ground-Based Measurements of Nitric Acid

KAZUYUKI KITA

Department of Environmental Sciences, Faculty of Science, Ibaraki University, Mito, Japan

YU MORINO, YUTAKA KONDO, YUICHI KOMAZAKI, NOBUYUKI TAKEGAWA, AND YUZO MIYAZAKI

Research Center for Advanced Science and Technology, University of Tokyo, Tokyo, Japan

JUN HIROKAWA

Graduate School of Environmental Earth Science, Hokkaido University, Sapporo, Japan

SHIGERU TANAKA

Department of Applied Chemistry, Faculty of Science and Technology, Keio University, Tokyo, Japan

THOMAS L. THOMPSON, RU-SHAN GAO, AND DAVID W. FAHEY

NOAA/Aeronomy Laboratory, Boulder, Colorado

(Manuscript received 5 May 2005, in final form 29 December 2005)

ABSTRACT

A chemical ionization mass spectrometer (CIMS) instrument has been developed for high-precision measurements of gaseous nitric acid (HNO_3) specifically under high- and variable-humidity conditions in the boundary layer. The instrument's background signals (i.e., signals detected when HNO_3-free air is measured), which depend on the humidity and HNO_3 concentration of the sample air, are the most important factor affecting the limit of detection (LOD). A new system to provide HNO_3-free air without changing both the humidity and the pressure of the sampled air was developed to measure the background level accurately. The detection limit was about 23 parts per trillion by volume (pptv) for 50-s averages. Field tests, including an intercomparison with the diffusion scrubber technique, were carried out at a surface site in Tokyo, Japan, in October 2003 and June 2004. A comparison between the measured concentrations of HNO_3 and particulate nitrate indicated that the interference from particulate nitrate was not detectable (i.e., less than about 1%). The intercomparison indicated that the two independent measurements of HNO_3 agreed to within the combined uncertainties of these measurements. This result demonstrates that the CIMS instrument developed in this study is capable of measuring HNO_3 mixing ratios with the precision, accuracy, and time resolution required for atmospheric science.

1. Introduction

Nitric acid (HNO_3) plays important roles in ozone (O_3) chemistry and aerosol formation in the troposphere. HNO_3 is produced via the oxidation of nitrogen dioxide (NO_2) by hydroxyl (OH) radical in the daytime:

$$\text{(R1)} \quad NO_2 + OH + M \rightarrow HNO_3 + M,$$

where M represents a third body (e.g., N_2 or O_2). Following the oxidation of NO_2 to produce N_2O_5 at night, HNO_3 is formed by hydrolysis of N_2O_5 (e.g., Tie et al. 2003; Takegawa et al. 2004):

$$\text{(R2)} \quad N_2O_5 + H_2O(s) \rightarrow 2HNO_3(s),$$

where (s) denotes a species on the surface of an aerosol. In the lower troposphere, HNO_3 rarely returns to NO_x via reaction with OH or photolysis because it is rapidly removed from the atmosphere (its lifetime is about a day or less) by deposition to the ground and/or uptake

Corresponding author address: Kazuyuki Kita, Faculty of Science, Ibaraki University, 2-1-1 Bunkyo, Mito 310-8512, Japan.
E-mail: kita@mx.ibaraki.ac.jp

into the clouds. Therefore, the formation of HNO_3 results in a net loss of NO_x, terminating the photochemical production of O_3.

In addition to these processes, HNO_3 co-condenses with gas-phase ammonia (NH_3) to form nonrefractory ammonium nitrate (NH_4NO_3) aerosol, most efficiently under low-temperature and high-humidity conditions (e.g., Seinfeld and Pandis 1998)

$$\text{(R3)} \quad HNO_3 + NH_3 \rightarrow NH_4NO_3(s).$$

NH_4NO_3 is one of the major components of urban aerosol (e.g., Kaneyasu et al. 1999; Moya et al. 2001; Metzger et al. 2002). HNO_3 also reacts with sea-salt particles to yield particulate sodium nitrate ($NaNO_3$) and gaseous hydrogen chloride (HCl). This reaction is believed to be important for the removal of reactive nitrogen (e.g., Davies and Cox 1998; Spokes et al. 2000) and the loss of chlorine from sea-salt particles.

Numerous attempts have been made to measure HNO_3 accurately. The conventional techniques for measuring HNO_3 are the filter and denuder tube methods (e.g., Heubert and Lazrus 1978; Shaw et al. 1982), which have time scales of 10 min to hours. A more improved method, the mist-chamber-ion chromatography technique, can measure HNO_3 within a few minutes and has been used extensively for aircraft measurements (Talbot et al. 1997, 2000). It has been reported that the evaporation of aerosol NH_4NO_3 from filters may cause uncertainty in the measurements (Fehsenfeld et al. 1998). Recently, the chemical ionization mass spectrometer (CIMS) technique has been adopted to measure HNO_3 with high precision and good time resolution, on the order of 10 s or less. Although some early CIMS HNO_3 measurements (e.g., Knop and Arnold 1985) could be susceptible to interference from water vapor and other odd nitrogen species, newly developed instruments using new chemical schemes have lessened this problem (Huey et al. 1998; Mauldin et al. 1998; Miller et al. 2000; Neuman et al. 2000, 2002; Zondlo et al. 2003). However, because background levels in the measurements may depend on humidity, there is still a need to establish the accuracy and reliability of HNO_3 measurements at low concentrations in the humid boundary layer.

We have developed a CIMS system dedicated to the accurate measurement of HNO_3 under high- and variable-humidity conditions in the boundary layer. Important factors influencing the sensitivity and accuracy of the measurements have been identified by laboratory experiments. This CIMS instrument was successfully deployed for ground-based HNO_3 measurements in Tokyo, Japan. The CIMS data obtained during these measurements were compared with those simultaneously measured by a diffusion scrubber coupled with an ion chromatograph (DS-IC). Here we describe the CIMS instrument, results obtained in the laboratory, and the results of the comparison.

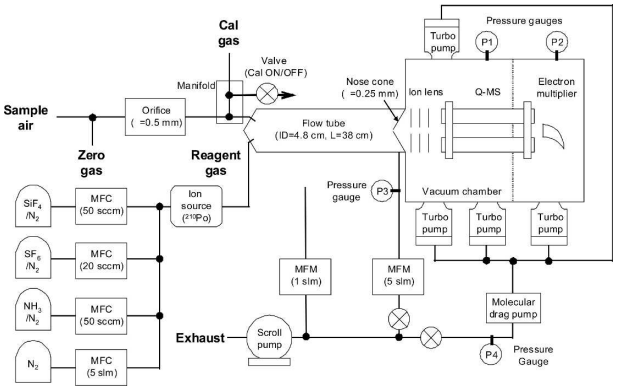

FIG. 1. Schematic diagram of the HNO_3 CIMS instrument developed in this study. Here MFM, MFC, Φ, ID, and L denote the mass flowmeter, the mass flow controller, the orifice (hole) diameter, the inner diameter of the tube, and the length, respectively.

2. Instrument description

Figure 1 is a schematic diagram of the CIMS instrument, which consists of an inlet, ion source, vacuum chamber, quadrupole mass spectrometer, HNO_3 calibration source, pumps, gas supply, and electronics including a computer (not shown). The CIMS systems developed in the National Oceanic and Atmospheric Administration (NOAA) Aeronomy Laboratory were used as a starting point for this new development (Huey et al. 1998; Neuman et al. 2000, 2002), and details of the instrument design were presented elsewhere (Neuman et al. 2000, 2002). Only a brief outline of this instrument is presented here. The reaction of HNO_3 with SiF_5^- reagent ions,

$$\text{(R4)} \quad SiF_5^- + HNO_3 \leftrightarrow SiF_5^- \cdot HNO_3,$$

has been adopted in these systems because of the selective detection of HNO_3 (Huey and Lovejoy 1996) and a relatively simple instrument design (Huey et al. 1998; Neuman et al. 2000). If the reaction time and temperature are such as to ensure the thermal equilibrium of the reaction (R4), the number density of the cluster ion, $[SiF_5^- \cdot HNO_3]$, is proportional to the product of the HNO_3 number density, $[HNO_3]$, and the reagent ion number density, $[SiF_5^-]$. The SiF_5^- reagent ions are produced by flowing the reagent gas, a mixture of N_2, SiF_4, and SF_6, through the ^{210}Po radioactive ion source tube. The reagent ions and the sample air are mixed in the flow tube. The flow rates of the gases and the temperature and pressure in the flow tube were

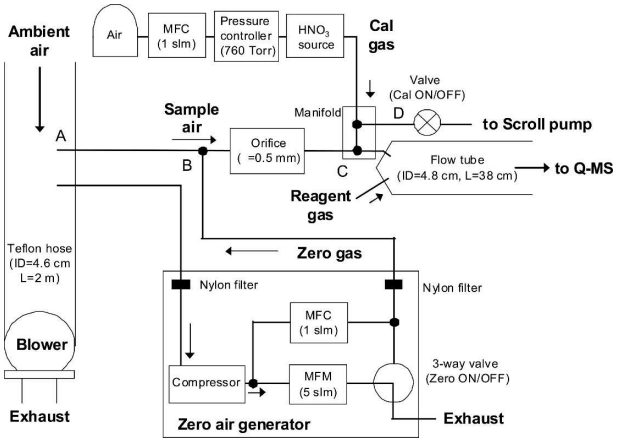

FIG. 2. Schematic design of the inlet with the calibration gas source and the zero gas generator.

optimized to maximize the sensitivity, as discussed in section 3.

The ions produced in the flow tube are extracted to a two-stage, cylindrical aluminum vacuum chamber. In this chamber, most ions are guided to the quadrupole mass filter by ion lenses, and the ions sieved out there are detected by a continuous dynode electron multiplier. The signal pulses from the electron multiplier are amplified, and then are counted and recorded by a computer, which also controls the instrument operations.

The design of the inlet for sampling the ambient air is crucial for measuring HNO_3 because HNO_3 is easily absorbed onto solid surfaces, including the inlet wall. Figure 2 is a schematic of the inlet. Most inlet surfaces in contact with the sampled air are made of perfluoroalkoxy (PFA) Teflon, with the remaining surfaces made of polytetrafluoroethylene (PTFE) Teflon. The ambient air is sampled through a 2-m-long straight PFA hose with a 4.6-cm inner diameter (ID). Starting outside at a point 1.4 m from the building wall, the ambient air is drawn through this hose at a flow rate of 1200 standard liters per minute (slm) by using a blower (MB-1665-B, Oriental Motor Co. Ltd., Tokyo, Japan). From the center of the hose, at about 1.9 m from the entry of the hose (A in Fig. 2), a small portion of the ambient air is drawn up into the flow tube at a flow rate of 2.0 slm by way of a 6.35-mm outer diameter (OD) PFA tube, a PTFE orifice (0.5-mm ID) for creating a pressure drop, and a PTFE manifold block for the calibration. The pressure downstream of the orifice is almost the same as that in the flow tube. The length of the PFA tube between point A and the orifice is about 8 cm, and that between the orifice and the entry port of the flow tube including the manifold is about 17 cm. All of these parts are heated to 35°C to minimize the HNO_3 loss (Kondo et al. 1997; Neuman et al. 1999).

The CIMS is periodically calibrated for HNO_3 observation. During calibration, sensitivity is measured by adding HNO_3 calibration gas to the sample air in the manifold (C in Fig. 2). The HNO_3 calibration source used here is a permeation tube (SRT-005, KIN-TEK Laboratories, Inc., LaMarque, Texas), which is stored in a PTFE sleeve packed into an aluminum block. During laboratory experiments and field observations, the temperature, gas flow rate, and pressure around the permeation tube are always controlled to 40.0° ± 0.1°C, 20 ± 1 standard cubic centimeters per minute (sccm), and 1013 ± 6 hPa, respectively, by using a temperature controller, a mass flow controller, and a forward pressure controller with a crimp at the exit of the HNO_3 source. The continuous flow of the calibration gas from the source to a tee in the manifold through a short (~10 cm) and heated (~35°C) tube between them, reduces the influence of HNO_3 absorption on the walls between them and significantly improves the time response. The HNO_3 gas injection from the source was controlled by closing and opening the solenoid valve (D in Fig. 2; Neuman et al. 2000). The ion signal responded to almost 100% within 2 s after closing or opening this valve (cf. Fig. 5 in Neuman et al. 2000), indicating that the absorption and desorption of HNO_3 on surfaces downstream of point C do not affect the time response of this instrument significantly. The ambient humidity can affect the sensitivity slightly because of the formation of the $SiF_5^- \cdot (H_2O)_n$ cluster ions in the flow tube. Because the flow rate of the calibration gas is much smaller (about 1%) than that of the sampled air, the humidity in the flow tube does not change during the calibration significantly.

The background level of the CIMS is determined from the count rate for $SiF_5^- \cdot HNO_3$ ions appearing when sampling HNO_3-free air (zero gas). Because it is very likely that the background level depends on the humidity of the sampled air, pure air from gas bottles cannot be used as the zero gas. To provide the zero gas, HNO_3 is removed from the ambient air by passing it through two nylon filters, which absorb HNO_3 almost completely without loss of H_2O. The loss rate of HNO_3 at one nylon filter was measured, confirming that it was greater than 99%. The background level is periodically measured by overflowing the inlet line with this zero gas at a point just upstream of the orifice (B in Fig. 2) at a flow rate of 4 slm, which exceeds the flow rate of the sampled air (2 slm), without a change of the inlet line pressure. It is significant to keep the inlet line pressure constant because the flow tube pressure, with which the sensitivity varies, depends on it, as shown in the next section. In addition, the zero gas is supplied at a low flow rate (50 sccm), even during the measurement

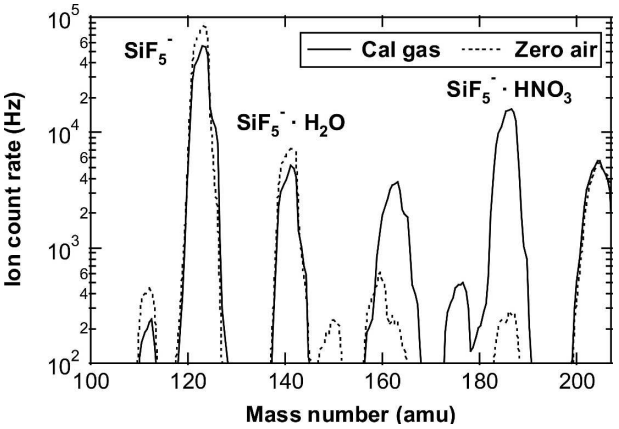

FIG. 3. Sample mass spectra obtained from the developed CIMS instrument. The dotted line was acquired when zero gas (Zero air) was sampled, and the solid line was acquired when the zero gas mixed with cal gas (Cal gas) was sampled.

of ambient HNO_3, to minimize absorption of HNO_3 by the PFA tube for injecting the zero air.

Figure 3 compares sample mass spectra obtained by this instrument during the calibration and the sampling of zero gas at about 1200 local time (LT) on 30 September 2003. The H_2O mixing ratio was 0.8%, and the HNO_3 mixing ratio was about 10 ppbv during the calibration. The SiF_5^- ions, at 123 atomic mass units (amu), are the most abundant ion. The $SiF_5^- \cdot HNO_3$ cluster ions, at 186 amu, are unambiguously identified, and their count rate was largely enhanced during the calibration. Because of the desorption of HNO_3 from the wall, some $SiF_5^- \cdot HNO_3$ ion signals (background signals) remained during the sampling of zero gas. During the measurements, the full-width half-maximum (FWHM) of this cluster ion peak is tuned to 2~3 amu. The addition of HNO_3 also increases the $SiF_4^- \cdot NO_3$ (166 amu) ions and the NO_3^- ions (62 amu). The NO_3^- ion count rate is less than 1000 (not shown). The peak at 205 amu is tentatively identified as $Si_2F_7O^-$ ion. The presence of H_2O generates $SiF_5^- \cdot (H_2O)_n$ ($n = 1, 2, \ldots$) cluster ions. The count rates of $SiF_5^- \cdot (H_2O)$ ions were comparable to those of $SiF_5^- \cdot HNO_3$ ions, suggesting possible interference by water vapor due to a competitive reaction with the reagent ion.

3. Laboratory experiments

The assembled CIMS instrument was tuned in the laboratory to increase the sensitivity and decrease the background level, thus maximizing the signal-to-noise (SN) ratio. The sensitivity and time response of this instrument was measured by using the HNO_3 calibration source. The sensitivity S of the instrument is given by $S = C_{net}/\chi(HNO_3)$, where C_{net} is the net increase of the $SiF_5^- \cdot HNO_3$ ion count rate when the calibration gas was injected, and $\chi(HNO_3)$ is that of the HNO_3 mixing ratio by addition of the calibration gas. When the HNO_3 calibration gas was injected from the tip of the sampling tube (A in Fig. 2) instead of the calibration port (C in Fig. 2), a 90% and 95% response of the ion signal were attained within 10 and 20 s after the injection, respectively, and the S value reasonably agreed with that obtained from the injection from port C. The 90% time response for the zero gas was also attained within 10 s after its injection. These results show that the 90% time response of this instrument is better than 10 s, and that the absorption and desorption of HNO_3 in the sampling tube between A and C were insignificant. Although the influences of the absorption and desorption of HNO_3 by the inlet Teflon hose have not been measured, it is probably insignificant considering the large flow rate and relatively large inner diameter of the hose, as suggested in the next section.

TABLE 1. Significant parameters to determine the SN ratio and their optimal values adopted in this CIMS instrument.

Parameter	Optimal value	Unit
N_2 flow rate in the reagent gas	2	slm
SiF_4/N_2* flow rate in the reagent gas	10	sccm
SF_6/N_2* flow rate in the reagent gas	10	sccm
Mixing ratio of NH_3 in the reagent gas	0.13	%
Temperature of the flow tube	5 ± 0.2	°C
Pressure in the flow tube	22.7 ± 0.3	hPa
Ion lens voltage at the first stage	10	V
Bias voltage	40	V

* Mixing ratios of SiF_4 in the SiF_4/N_2 gas mixture and SF_6 in the SF_6/N_2 gas mixture are 0.46 and 0.42 ppm by volume (ppmv), respectively.

Laboratory experiments showed that the sensitivity and the background signal depend on the flow rates of the reagent gases, the temperature of the flow tube, and the pressure in it, as shown below. Also, the sensitivity slightly depends on the ion lens voltages and DC bias voltage, which is supplied to the four mass filter rods equally for guiding ions to the quadrupole mass filter. The $SiF_5^- \cdot HNO_3$ ion signal increased as these voltages increased, although it did not increase or decrease when these voltages exceeded their optimal values. Table 1 lists significant parameters affecting the SN ratio and their optimal values determined in the laboratory experiments for this CIMS instrument.

The sensitivity depends on the number density of the reagent SiF_5^- ion, which varies with the flow rates of gases included in the reagent gas. The reagent ion density was nearly proportional to both the total (mostly N_2) flow rate of the reagent gas and the SiF_4/N_2 gas

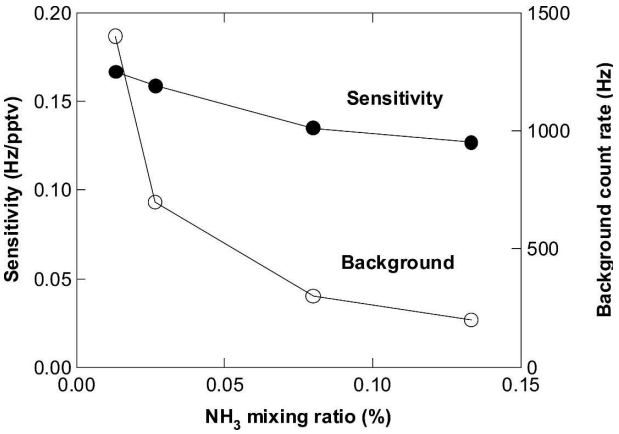

FIG. 4. Changes in sensitivity and background signal as functions of the mixing ratio of NH_3 added in the ion source gas.

flow rate in the reagent gas, although it stayed the same or decreased when these flow rates exceeded their optimal values. Mixing of NH_3 with the reagent gas reduces the background signal significantly because it converts the HNO_3 absorbed on the inner wall of the flow tube to the solid NH_4NO_3 (Huey et al. 1998; Neuman et al. 2000). Figure 4 shows the sensitivity and the background signals as a function of the NH_3 mixing ratio. The background signal decreased by more than 85% at an NH_3 mixing ratio of 0.13%. However, the sensitivity dropped significantly (by more than 20%) if the NH_3 mixing ratio exceeded this value because NH_3 can react with SiF_4 in the reagent gas and with HNO_3 in the sampled air.

It should be noted that the sensitivity depends significantly on the temperature in the flow tube because the equilibrium constant of (R4) depends on the temperature (Huey and Lovejoy 1996; Huey et al. 1998). Figure 5a shows the sensitivity and the background signal measured as functions of the flow tube temperature. The temperature was regulated by circulating cooled water around the flow tube. The sensitivity decreased with increasing temperature, especially above 20°C (not shown). At the same time, the background signal significantly increased with increasing temperature because the release of HNO_3 from the flow tube wall increases with the temperature. These results indicate that the cooling of the flow tube can strongly improve both the sensitivity and the background level. Figure 5b shows that the sensitivity and the background signal decreased with increasing flow tube pressure, probably because of increased collisional loss of the $SiF_5^- \cdot HNO_3$ ion at the wall and reduced release of HNO_3 from the wall at higher pressures. The sensitivity drop may be attributed also to the decrease in the ion optics transmittance, including that of the mass filter, by a pressure

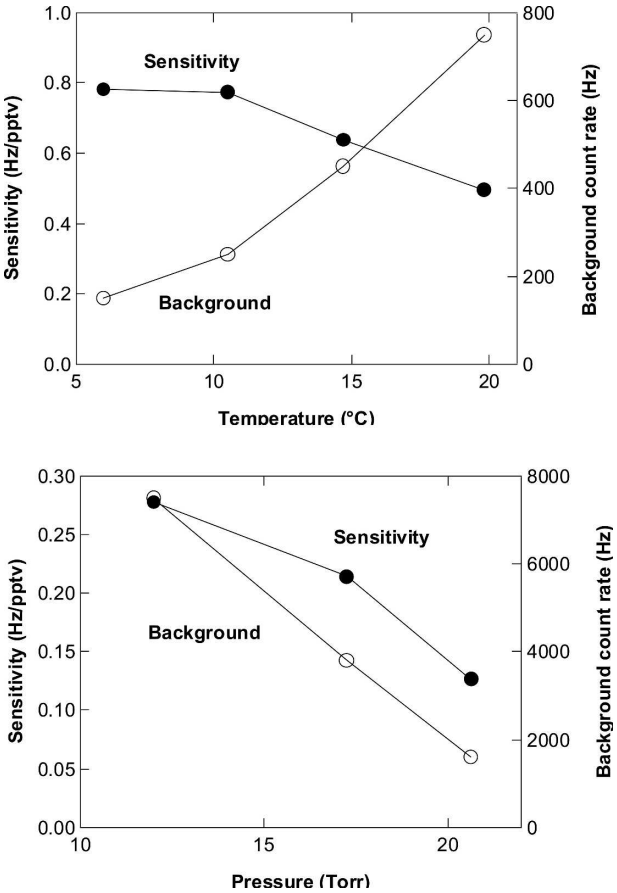

FIG. 5. Same as in Fig. 4, but for (top) the flow tube temperature and (bottom) the flow tube pressure.

increase. The temperature and the pressure of the flow tube were maintained at 5° ± 0.2°C and 17 ± 0.2 Torr (22.4 ± 0.3 hPa), respectively, to maximize the SN ratio.

Under the optimized conditions as explained above, the $SiF_5^- \cdot HNO_3$ ion signals increase linearly with the HNO_3 concentration at mixing ratios of less than 12 ppbv, resulting in a sensitivity of 1.20 ± 0.02 Hz $(pptv)^{-1}$. This value is similar to that of other CIMS instruments, in which the ionization with SiF_5^- reagent ions has been used (Huey et al. 1998; Neuman et al. 2000, 2002; Furutani and Akimoto 2002). The ion signals slightly depart from linearity at HNO_3 mixing ratios exceeding 12 ppbv. This nonlinearity is due mainly to a significant decrease in the reagent ion concentration by the reaction with HNO_3. For the present study, nonlinearity was not a serious problem because the HNO_3 mixing ratios in ambient air in Tokyo were less than 12 ppbv, well within the linear region. Temporal variation of the sensitivity is compensated by frequent calibration, which was made at HNO_3 mixing ratios of about 10 ppbv, during the observation. Because the

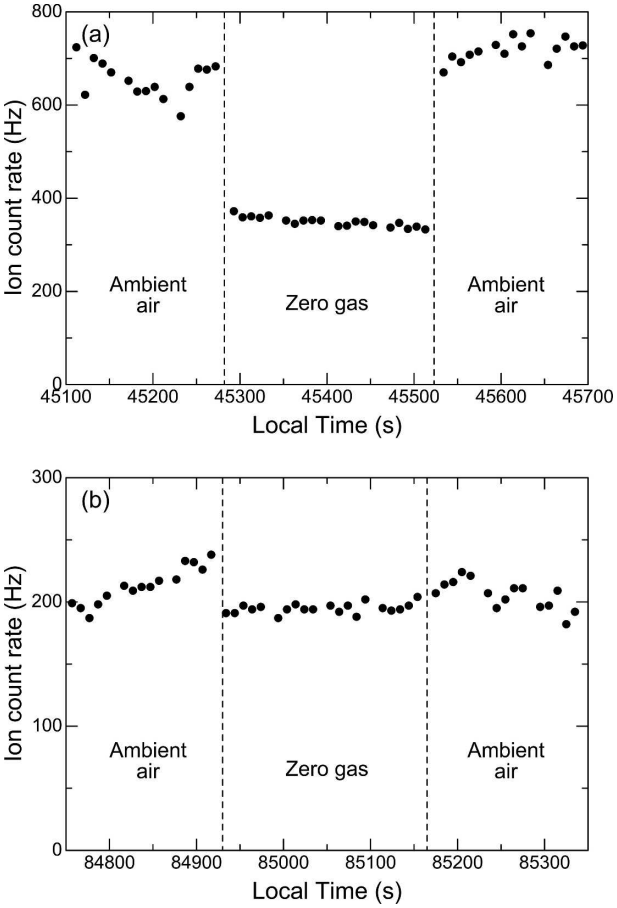

FIG. 6. The $SiF_5^- \cdot HNO_3$ ion signal response to the zero gas injection (a) during the day and (b) at night on 11 May 2003. Closed circles are 10-s average data. The dotted lines denote the start and end of the zero gas injection.

sensitivity depends on the reagent ion density, this density is monitored at 10-min intervals to detect significant variations. However, unlike the case with similar CIMS instruments (Huey et al. 1998; Neuman et al. 2000), the SiF_5^- ion signal is not directly used to compensate its fluctuation in this instrument because the ion signal is so large that its uncertainty due to hysteresis and nonlinearity is not negligible.

Accurate determination of the background level is crucial for HNO_3 measurements at low concentrations. The precision and the detection limit of this instrument are determined by the fluctuation of the background signal of the $SiF_5^- \cdot HNO_3$ ion. The primary source of this background signal is considered to be the desorption of gaseous HNO_3 and particulate nitrate absorbed on the inner walls of the inlet and flow tube. Figures 6a,b show background signals measured in the daytime and nighttime in Tokyo on 11 May 2003, showing the representative background level and its fluctuation at high and low concentrations of ambient HNO_3. While the average background level is approximately proportional to the HNO_3 concentration in the sampled air, its fluctuation did not change significantly. The 50-s average background signal and standard deviation (σ_B) from it at 45 410 s (HNO_3 ~820 pptv) and at 85 050 s (HNO_3 ~40 pptv) in Figs. 6a,b were 344 ± 5 Hz and 195 ± 5 Hz, respectively. The precision is given by average $2\sigma_B$ values for 50-s averages of 10-s integrated data, and is about 9 pptv (17 pptv) at HNO_3 mixing ratios of about 50 pptv (1 ppbv). The background level responds very slowly to variations in the ambient HNO_3 concentration. A 4-min injection of the calibration gas (HNO_3 ~10 ppbv) did not affect the background level, even when the ambient HNO_3 concentration was very low (<50 pptv). The background level was measured for 4 min at 1-h intervals, and was interpolated between measurements. Another uncertainty is caused by errors in this interpolation. This uncertainty (δ_B) is estimated to be less than a half of the average difference between two successive measured values of the background signal: 6.4 and 16 pptv at HNO_3 mixing ratios of 50 and 1 ppbv, respectively. The limit of detection (LOD) for HNO_3 mixing ratios of less than 50 pptv is given by $3(\sigma_B^2 + \delta_B^2)^{1/2}$ and is estimated to be about 23 pptv.

TABLE 2. Errors of the CIMS instrument in the HNO_3 measurement at concentrations of 50 and 1 ppbv. Integration time is 50 s.

Error source	Percent (at 50 pptv)	Percent (at 1 ppbv)
Systematic errors		
HNO_3 emission rate from the permeation tube	6	6
Gas flow rates	3	3
Residual HNO_3 in the zero gas	<2	<2
Influence by water vapor	<5	<5
Random errors		
Uncertainty in the calibration signal	2	2
Uncertainty in the background level	16	2
Total error	<19	<9

Table 2 summarizes the sources of uncertainties in the HNO_3 measurement with this CIMS instrument. Systematic errors in this measurement are mostly originated from that in the HNO_3 emission rate of the calibration source and from that in the sample airflow rate. The HNO_3 emission rate from the calibration source was measured in the laboratory with an ion chromatograph (IC) 3 times between June 2003 and April 2005. The average HNO_3 emission rate measured with the IC was 73.5 ng $(min)^{-1}$, consistent with the value of 72 ng $(min)^{-1}$ provided by the manufacturer. The precision and accuracy of the IC measurement were evaluated to

be 2% and 6%, respectively. The uncertainties in the flow rates of the sampled air and calibration gas were estimated to be less than 3%. The error resulting from interference by water vapor is discussed in the next section. The uncertainty associated with the determination of the background level, $(\sigma_B^2 + \delta_B^2)^{1/2}$, was 19 pptv, about 2% at a HNO_3 mixing ratio of 1 ppbv. The standard deviation of the calibration signal was about 2%. Considering these uncertainties, the overall accuracy of the measurement was estimated to be about ±9% (±19%) at a HNO_3 mixing ratio of 1 ppbv (50 pptv).

4. Field observation and intercomparison with the DS-IC instrument

Using this instrument, surface HNO_3 concentrations were measured at the Research Center for Advanced Science and Technology (RCAST) of the University of Tokyo, located at Komaba (35°40′N, 139°40′E) in west-central Tokyo, Japan, during the Integrated Measurement Program for Aerosol and Oxidant Chemistry in Tokyo (IMPACT) campaigns in 2003–04. Ambient air was sampled on the fourth floor (about 12 m above ground level) of one of the buildings at RCAST. The HNO_3 was measured simultaneously with other gaseous reactive nitrogen components (NO, NO_2), nitrate (NO_3^-) in fine aerosol particles (diameter less than 1 μm), ozone, and meteorological parameters. Both NO and NO_2 were measured with a chemiluminescence instrument (Kondo et al. 1997; Nakamura et al. 2003), and NO_3^- was measured with an aerosol mass spectrometer (AMS) instrument (Jayne et al. 2000; Allan et al. 2003). During IMPACT, NO_3^- in fine particles was also measured with a (particle-into-liquid collector) PILS-IC instrument (Weber et al. 2001), and the two measurements were generally consistent with each other (Takegawa et al. 2005).

Although the HNO_3 measurement with CIMS adopting the SiF_5^- reagent ion is not sensitive to NO_2 and particulate NO_3^- (Huey and Lovejoy 1996; Neuman et al. 2003), interference due to the conversion of these species to HNO_3 in the instrument should be tested. For example, evaporation of particulate NO_3^- at the inner wall of the inlet tube heated to 35°C may produce excess HNO_3. Figure 7 compares times series of HNO_3, NO_2, and NO_3^- in fine particles from 10 to 12 October 2003. Throughout each night, while the concentrations of NO_2 and NO_3^- often exceeded 30 and 1 ppbv, respectively, the measured HNO_3 concentrations were small (<80 pptv). Considering that detected HNO_3 concentrations were less than 30 pptv when the NO_2 and NO_3^- concentrations were 28–35 and 2.0–2.5 ppbv, interference from these species is estimated to be less than 0.1% and 1.2% of the NO_2 and NO_3^- concentrations, respectively.

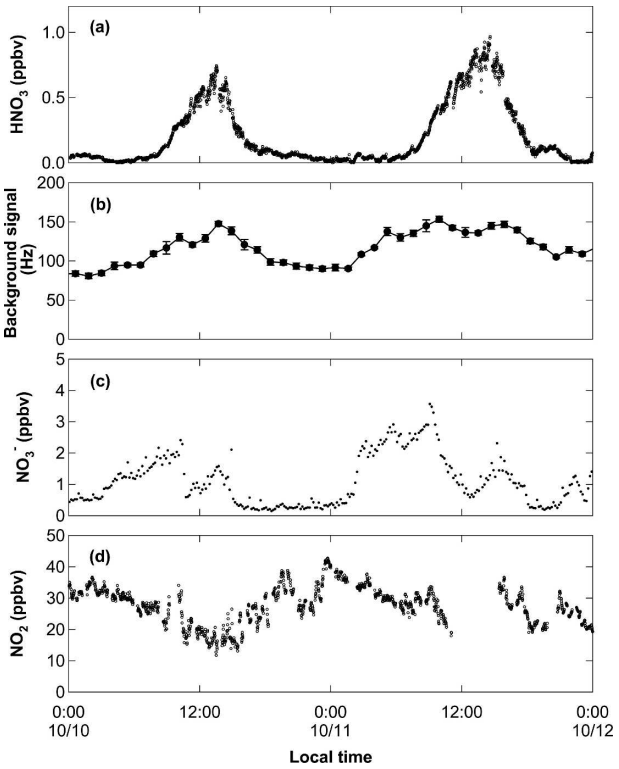

FIG. 7. Time series of the measured mixing ratios of (a) HNO_3, (c) NO_3^- in fine particles, and (d) NO_2 between 10 and 12 Oct 2003. (b) Time series of the background level for the HNO_3 measurement.

The background level is affected by the ambient HNO_3 and NO_3^- concentrations. It is likely that the background level and the sensitivity vary considerably with the humidity of the sampled air in the humid boundary layer, although previous works (Huey et al. 1998; Neuman et al. 2000, 2003) showed that the sensitivity of similar CIMS instruments did not depend on humidity significantly. Errors associated with the variation of these species were minimized by frequent calibration without a change in humidity. During the IMPACT campaigns, the calibration was conducted at regular 1-h intervals. Figure 7b shows a time series of the background level. When both the ambient HNO_3 and NO_3^- concentrations were low (less than 0.1 and 1 ppbv, respectively), the background level was stable; the average difference between two successive measured values of the background signal was 10.3 pptv. Although the background level increased with the ambient HNO_3 and NO_3^- concentrations, the increase in the background level was about 10% of that in the ambient HNO_3 and NO_3^- concentrations. These results show that the error due to change in the background

level is consistent with the estimation in section 3. Considering changes in humidity between these intervals, errors due to those changes were estimated to be 5% at most.

An intercomparison of the two HNO_3 measurements with the independent techniques was carried out in October 2003 and June 2004 during IMPACT: CIMS and a diffusion scrubber coupled with an ion chromatograph (DS-IC). The DS-IC instrument used here is an improved version of that developed by Komazaki et al. (1999, 2002). The DS-IC consists of a 30-cm porous PTFE tube concentrically mounted within a Pyrex glass tube. Deionized water, which serves as the scrubbing solution for HNO_3, flows in the annular space between the inner and outer tubes in a direction opposite that of the gas. In the present study, ambient air was sampled with the DS-IC at 1.0 slm through a 35°C heated PFA tube (6.35-mm OD, 15-cm length) from a common sampling inlet for CIMS measurements. Ambient air and HNO_3-free air, which was produced by removing HNO_3 from the ambient air using nylon filters, were alternately sampled to make quantitative corrections for the background NO_3^- in the diffusion scrubber. The scrubbing solution was continuously preconcentrated on a concentrator column (Metrosep Anion IC preconcentration, Metrohm) at 1.5 mL min^{-1} during the 20-min sample air collection period and for an additional 5 min for complete preconcentration of NO_3^- in the scrubbing solution prior to ion chromatographic analysis. The overall sampling time interval was 1 h. The DS-IC was calibrated with the same HNO_3 permeation tube as that used for the CIMS, thus systematic error due to calibration can be ignored in this comparison. The background level was regularly measured at 6-h intervals in October 2003, and was measured at 1-h intervals in June 2004, to improve the accuracy at low HNO_3 concentrations. The lower detection limit (3σ of the blank values of NO_3^-) of HNO_3 was improved to be 20 pptv for a 20-L air sample (20-min integration) in June 2004. The absolute accuracy was estimated to be better than 30% at a HNO_3 mixing ratio of 1 ppbv, considering uncertainties in the sampling efficiency of HNO_3 in the DS, ion chromatographic analysis, and calibration.

Figure 8 shows the temporal variations of the HNO_3 mixing ratios measured with the CIMS and DS-IC instruments between 3 and 6 June 2004. The two HNO_3 measurements agree quite well in diurnal variation. The diurnal variation was similar to that of O_3, suggesting that it is driven principally by the photochemical production via (R1) and rapid removal by dry deposition to the surface and by adsorption onto aerosols. The compact correlation between the two species suggests

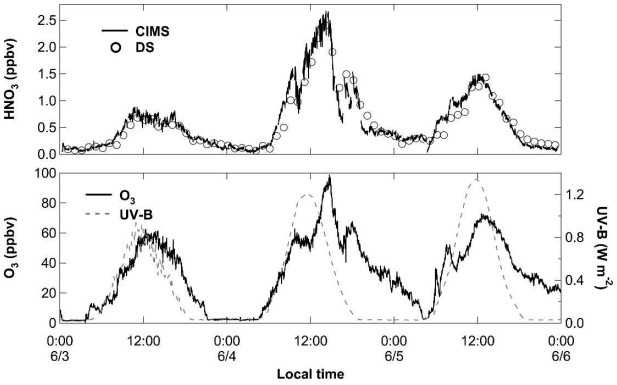

FIG. 8. Time series of the HNO_3 mixing ratios measured with (top) the CIMS and DS-IC instruments and (bottom) the ozone mixing ratio and the UV-B intensity between 3 and 5 Jun 2004.

that the formation of HNO_3 was dominantly governed by the O_3 concentration, and that the time response of the HNO_3 measurement was similar to that of the O_3 measurement (12 s).

Figure 9 compares HNO_3 concentrations measured with the CIMS and DS-IC during two periods (October 2003 and June 2004). The two measurements generally agreed with each other to within the combined uncertainties of these measurements (31% at a HNO_3 mixing ratio of 1 ppbv) and correlated quite well, with $R^2 =$ 0.91–0.93 and a slope of 0.92–0.94. No significant bias or offset was found between them, considering the accuracy of the two instruments. This comparison demonstrates a strong self-consistency between the two HNO_3 measurements, consistent with the estimate made in section 3 for the CIMS.

5. Summary

A CIMS instrument has been developed for the precise measurement of HNO_3, specifically under high and variable humidity conditions in the boundary layer. The sensitivity and the background level of this instrument depended on the temperature of the flow tube. By lowering this temperature down to 5°C from 20°C, the sensitivity increased by 30% while the background level decreased by 80%. This, together with the optimization of other instrument parameters, including the ion source gas flow, led to a precision of 9 pptv for 50-s averages. The 90% response of the HNO_3 measurement was found to be faster than 10 s.

The accurate determination of background level is crucial for measuring low concentrations of HNO_3 accurately. The background level of this instrument increased with the increases in the humidity and HNO_3 concentration of the sample air. A new system to pro-

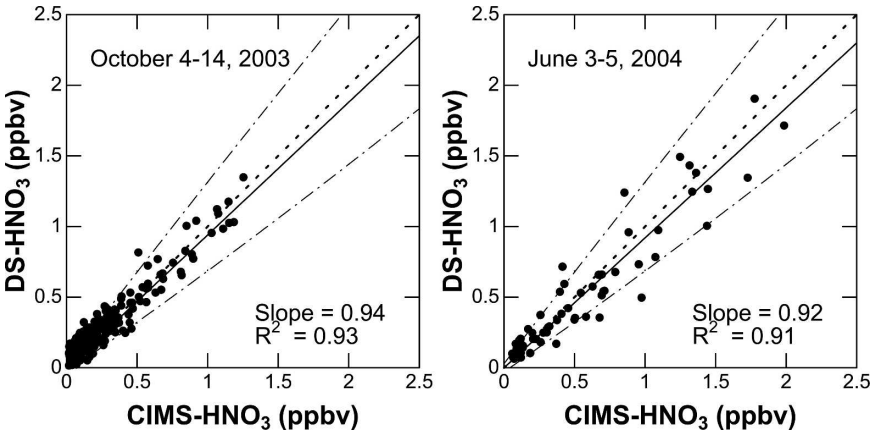

FIG. 9. Comparison of the HNO_3 measurements from the CIMS instrument and the DS-IC instrument (left) between 4 and 14 Oct 2003 and (right) between 3 and 5 Jun 2004. The solid line corresponds to a linear least squares fit to the data, and the dotted line indicates the 1:1 correspondence. The dot–dashed lines show the combined error range of the two measurements.

vide HNO_3-free air without changes both in humidity and pressure enabled accurate and frequent measurement of the background level, leading to a detection limit as low as 23 pptv at a HNO_3 mixing ratio of less than 50 pptv for 50-s averages of 10-s integrated data. The accuracy of this instrument is estimated to be about 9% at a HNO_3 mixing ratio of 1 ppbv, considering the uncertainties in calibration and fluctuations in the background level.

This instrument was used during intensive ground-based observations made in Tokyo in 2003 and 2004. HNO_3 (particulate nitrate) concentrations were often 0–30 pptv (2–3 ppbv) at night, indicating that interference from particulate nitrate was negligible. The upper limits of interference from NO_2 and particulate nitrate are estimated to be less than 0.1% and 1.3%, respectively. HNO_3 measurement was intercompared between the CIMS instrument and the diffusion scrubber technique by sampling urban air in Tokyo in October 2003 and June 2004. The two measurements agreed with each other to within the combined uncertainties of these measurements. This demonstrated the overall validity of the HNO_3 measurements by CIMS.

Acknowledgments. This study was funded in part by the Ministry of Education, Culture, Sports, Science, and Technology of Japan with Special Coordination Funds for Promoting Science and Technology. The authors thank the following people: J. A. Neuman for his helpful information on the CIMS design; and M. Fukuda, T. Miyakawa, and N. Moteki for their help with the HNO_3 measurements during the IMPACT campaign.

REFERENCES

Allan, J. D., J. L. Jimenez, P. I. Williams, M. R. Alfarra, K. N. Bower, J. T. Jayne, H. Coe, and D. R. Worsnop, 2003: Quantitative sampling using an Aerodyne aerosol mass spectrometer. 1. Techniques of data interpretation and error analysis. *J. Geophys. Res.,* **108,** 4090, doi:10.1029/2002JD002358.

Davies, J. A., and R. A. Cox, 1998: Kinetics of the heterogeneous reaction of HNO_3 with NaCl: Effect of water vapor. *J. Phys. Chem.,* **102A,** 7631–7642.

Fehsenfeld, F. C., L. G. Huey, D. T. Sueper, R. B. Norton, E. J. Williams, F. L. Eisele, R. L. Mauldin III, and D. J. Tanner, 1998: Ground-based intercomparison of nitric acid measurement techniques. *J. Geophys. Res.,* **103,** 3343–3354.

Furutani, H., and H. Akimoto, 2002: Development and characterization of a fast measurement system for gas-phase nitric acid with a chemical ionization mass spectrometer in the marine boundary layer. *J. Geophys. Res.,* **107,** 4016, doi:10.1029/2000JD000269.

Heubert, B. J., and A. L. Lazrus, 1978: Global tropospheric measurements of nitric acid vapor and particulate nitrate. *Geophys. Res. Lett.,* **5,** 557–580.

Huey, L. G., and E. R. Lovejoy, 1996: Reactions of $SiF5^-$ with atmospheric trace gases: Ion chemistry for chemical ionization detection of HNO3 in the troposphere. *Int. J. Mass Spectr. Ion Processes,* **155,** 133–140.

——, E. J. Dunlea, E. R. Lovejoy, D. R. Hanson, R. B. Norton, F. C. Fehsenfeld, and C. J. Howard, 1998: Fast time response measurements of HNO_3 in air with a chemical ionization mass spectrometer. *J. Geophys. Res.,* **103,** 3355–3360.

Jayne, J. T., D. C. Leard, X. Zhang, P. Davidovits, K. A. Smith, C. E. Kolb, and D. R. Worsnop, 2000: Development of an aerosol mass spectrometer for size and composition: Analysis of submicron particles. *Aerosol Sci. Technol.,* **33,** 49–70.

Kaneyasu, N., H. Yoshikado, T. Mizuno, K. Sakamoto, and M. Soufuku, 1999: Chemical forms and sources of extremely high nitrate and chloride in winter aerosol pollution in the Kanto Plain of Japan. *Atmos. Environ.,* **33,** 1745–1756.

Knop, G., and F. Arnold, 1985: Nitric acid vapour measurements

in the troposphere and lower stratosphere by chemical ionization mass spectrometry. *Planet. Space Sci.,* **33,** 983–986.

Komazaki, Y., Y. Hamada, S. Hashimoto, T. Fujita, and S. Tanaka, 1999: Development of an automated, simultaneous and continuous measurement system by using a diffusion scrubber coupled to ion chromatography for monitoring trace acidic and basic gases (HCl, HNO_3, SO_2, and NH_3) in the atmosphere. *Analyst,* **124,** 1151–1157.

——, S. Hashimoto, T. Inoue, and S. Tanaka, 2002: Direct collection of HNO_3 and HCl by a diffusion scrubber without inlet tubes. *Atmos. Environ.,* **36,** 1241–1246.

Kondo, Y., and Coauthors, 1997: The performance of an aircraft instrument for the measurement of NO_y. *J. Geophys. Res.,* **102,** 28 663–28 671.

Mauldin, R. L., III, D. J. Tanner, and F. L. Eisele, 1998: A new chemical ionization mass spectrometer technique for the fast measurement of gas phase nitric acid in the atmosphere. *J. Geophys. Res.,* **103,** 3361–3367.

Metzger, S., F. Dentener, M. Krol, A. Jeuken, and J. Lelieveld, 2002: Gas/aerosol partitioning. 2. Global modeling results. *J. Geophys. Res.,* **107,** 4313, doi:10.1029/2001JD001103.

Miller, T. M., and Coauthors, 2000: Chemical ionization mass spectrometer technique for the measurement of HNO_3 in air traffic corridors in the upper troposphere during the SONEX campaign. *J. Geophys. Res.,* **105,** 3701–3708.

Moya, M., A. S. Ansari, and S. P. Pandis, 2001: Partitioning of nitrate and ammonium between the gas and particulate phases during the 1997 IMADA-AVER study in Mexico City. *Atmos. Environ.,* **35,** 1791–1804.

Nakamura, K., and Coauthors, 2003: Measurement of NO_2 by the photolysis conversion technique during the Transport and Chemical Evolution over the Pacific (TRACE-P) campaign. *J. Geophys. Res.,* **108,** 4752, doi:10.1029/2003JD003712.

Neuman, J. A., L. G. Huey, T. B. Ryerson, and D. W. Fahey, 1999: Study of inlet materials for sampling atmospheric nitric acid. *Environ. Sci. Technol.,* **33,** 1133–1136.

——, and Coauthors, 2000: A fast-response chemical ionization mass spectrometer for in situ measurements of HNO_3 in the upper troposphere and lower stratosphere. *Rev. Sci. Instrum.,* **71,** 3886–3894.

——, and Coauthors, 2002: Fast-response airborne in situ measurements of HNO_3 during the Texas 2000 Air Quality Study. *J. Geophys. Res.,* **107,** 4436, doi:10.1029/2001JD001437.

——, and Coauthors, 2003: Variability in ammonium nitrate formation and nitric acid depletion with altitude and location over California. *J. Geophys. Res.,* **108,** 4557, doi:10.1029/2003JD003616.

Seinfeld, J. H., and S. P. Pandis, 1998: *Atmospheric Chemistry and Physics: From Air Pollution to Climate Change.* John Wiley & Sons, 1326 pp.

Shaw, R. W., R. K. Stevens, J. Bowermaster, J. W. Tesch, and E. Tew, 1982: Measurements of atmospheric nitrate and nitric acid: The denuder difference experiment. *Atmos. Environ.,* **16,** 845–853.

Spokes, L. J., S. G. Yeatman, S. E. Cornell, and T. D. Jickells, 2000: Nitrogen deposition to the eastern Atlantic Ocean: The importance of south easterly flow. *Tellus,* **52B,** 37–49.

Takegawa, N., and Coauthors, 2004: Removal of NO_x and NO_y in Asian outflow plumes: Aircraft measurements over the western Pacific in January 2002. *J. Geophys. Res.,* **109,** D23S04, doi:10.1029/2004JD004866.

——, and Coauthors, 2005: Characterization of an Aerodyne Aerosol Mass Spectrometer (AMS): Intercomparison with other aerosol instruments. *Aerosol Sci. Technol.,* **39,** 760–770.

Talbot, R. W., and Coauthors, 1997: Large-scale distributions of tropospheric nitric, formic, and acetic acids over the western Pacific basin during wintertime. *J. Geophys. Res.,* **102,** 28 303–28 313.

——, and Coauthors, 2000: Tropospheric reactive odd nitrogen over the South Pacific in austral springtime. *J. Geophys. Res.,* **105,** 6681–6694.

Tie, X., and Coauthors, 2003: Effect of sulfate aerosol on tropospheric NO_x and ozone budgets: Model simulation and TOPSE evidence. *J. Geophys. Res.,* **108,** 8364, doi:10.1029/2001JD001508.

Weber, R. J., D. Orsini, Y. Daun, Y.-N. Lee, P. J. Klotz, and F. Brechtel, 2001: A particle-into-liquid collector for rapid measurement of aerosol bulk chemical composition. *Aerosol Sci. Technol.,* **35,** 718–727.

Zondlo, M. A., R. L. Mauldin, E. Kosciuch, C. A. Cantrell, A. Christopher, and F. L. Eisele, 2003: Development and characterization of an airborne-based instrument used to measure nitric acid during the NASA Transport and Chemical Evolution over the Pacific field experiment. *J. Geophys. Res.,* **108,** 8793, doi:10.1029/2002JD003234.